https://doi.org/10.3311/PPee.38412

Periodica Polytechnica Electrical Engineering and Computer Science, 69(2), pp. 167–174, 2025

Numerical Simulation of the Thermal Behavior of a Lithium-ion Cell Pack with Various Thermal Dissipation Structure and the Addition of Phase Change Materials

Nour El Houda Korbaa[1*], Mohammed El Bachir Ghribi[1], Nadir Bouchetata[1], Ahmed Wahid Belarbi[1], Ghalem Bachir[2]

[1] Laboratory of Applied Power Electronics (LEPA), Department of Electrical Engineering, Faculty of Electrical Engineering, University of Sciences and Technology of Oran Mohamed-Boudiaf (USTOMB), El-Mnaouer, P. O. B. 1505, 31000 Bir El Djir, Oran, Algeria
[2] Laboratory of Sustainable Development of Electrical Energy (LDDEE), Department of Electrical Engineering, Faculty of Electrical Engineering, University of Sciences and Technology of Oran Mohamed-Boudiaf (USTOMB), El-Mnaouer, P. O. B. 1505, 31000 Bir El Djir, Oran, Algeria
* Corresponding author, e-mail: nourelhouda.korbaa@univ-usto.dz

Received: 25 September 2024, Accepted: 26 May 2025, Published online: 06 June 2025

Abstract

This study presents a transformative approach to passive thermal management in lithium iron phosphate ($LiFePO_4$) battery packs through geometrically optimized aluminum cooling structures. We investigate four distinct configurations - baseline (uncooled), unilateral side plate, inter-cell plates, and molded enclosure using experimentally validated COMSOL Multiphysics simulations under extreme 20C discharge conditions (50 A per cell). The most advanced design, featuring an aluminum mold surrounding 90% of each cell's height, achieves an unprecedented 11 °C reduction in peak temperature (from 66 °C to 55 °C) compared to conventional uncooled packs, while maintaining 99.1% of original power output (1107 W vs. 1118 W). This performance surpasses existing passive cooling methods and rivals many active systems, accomplished through three key innovations: 1. a patented snap-fit aluminum geometry that enhances heat transfer while simplifying assembly, 2. strategic material distribution that reduces thermal gradients by 32% compared to baseline, and 3. a cost-effective solution adding less than $1 per pack in material expenses. Furthermore, when combined with paraffin phase change material, the system demonstrates additional thermal buffering capacity, delaying critical temperature thresholds by 4.2 minutes during overload conditions. These findings provide battery designers with validated, scalable solutions that address the critical trade-offs between cooling performance, power output, and manufacturing complexity in next-generation energy storage systems.

Keywords

lithium-ion batteries, passive thermal management, aluminum heat sinks, phase change materials, battery temperature control, COMSOL simulation

1 Introduction

Recent advancements in lithium-ion battery technology have enabled significant improvements in energy density and efficiency, making these power sources indispensable for applications ranging from electric vehicles to grid storage [1–3]. However, a critical challenge persists in managing the thermal behavior of these batteries, particularly during high-current operations where excessive heat generation can lead to accelerated degradation or even catastrophic thermal runaway when temperatures exceed 60 °C [4–8]. Conventional thermal management approaches typically rely on active air-cooling systems [9–12] or phase change materials (PCMs) like paraffin [13–15], each presenting notable limitations. While air-cooling requires additional energy input and complex ducting systems, PCMs suffer from low thermal conductivity and volume change issues during phase transitions. Recent studies have explored alternative cooling structures using highly conductive materials like copper or silver [16], though their implementation remains constrained by cost and weight considerations. This study introduces an innovative approach to passive thermal management by systematically evaluating various aluminum-based

Cite this article as: Korbaa, N. E. H., Ghribi, M. E. B., Bouchetata, N., Belarbi, A. W., Bachir, G. "Numerical Simulation of the Thermal Behavior of a Lithium-ion Cell Pack with Various Thermal Dissipation Structure and the Addition of Phase Change Materials", Periodica Polytechnica Electrical Engineering and Computer Science, 69(2), pp. 167–174, 2025. https://doi.org/10.3311/PPee.38412

heat dissipation structures integrated within a lithium iron phosphate ($LiFePO_4$) battery pack. Our work distinguishes itself from previous research through its comprehensive comparison of four distinct aluminum configurations - including side plates, inter-cell spacers, and molded enclosures - combined with parametric analysis of PCM integration. Using COMSOL Multiphysics simulations [17] under extreme 20C discharge conditions (50 A current), we demonstrate that optimized aluminum geometries can reduce peak temperatures by up to 11 °C compared to baseline configurations, while maintaining favorable power output characteristics. The findings provide practical insights for battery pack designers seeking cost-effective thermal solutions that balance performance, weight, and manufacturability, particularly for applications where active cooling systems may be impractical. By quantifying the thermal performance benefits of specific aluminum structures and their synergies with PCM materials, this research advances the development of passive thermal management systems that can enhance both safety and longevity of lithium-ion battery packs.

2 Proposed structure

This study presents four experimentally validated thermal management configurations for 4S2P $LiFePO_4$ battery packs as shown in Fig. 1, systematically advancing prior work in [9, 12] while introducing critical innovations. The baseline Case 1 establishes reference performance using a conventional arrangement of 26650 cells (26 mm diameter × 65 mm height, 2.5 Ah capacity) with 2.6 mm air gaps and natural convection h = 30 W/m^2 K, consistent with assumption in [12]. Case 2 implements the simplest practical modification - a 2 mm thick aluminum 6061 plate (k = 237 W/(m·K) per ASTM B209/B209M-21a [18]) on one pack face, maintaining identical 2.6 mm spacing while providing unilateral cooling. Building on the limitations of

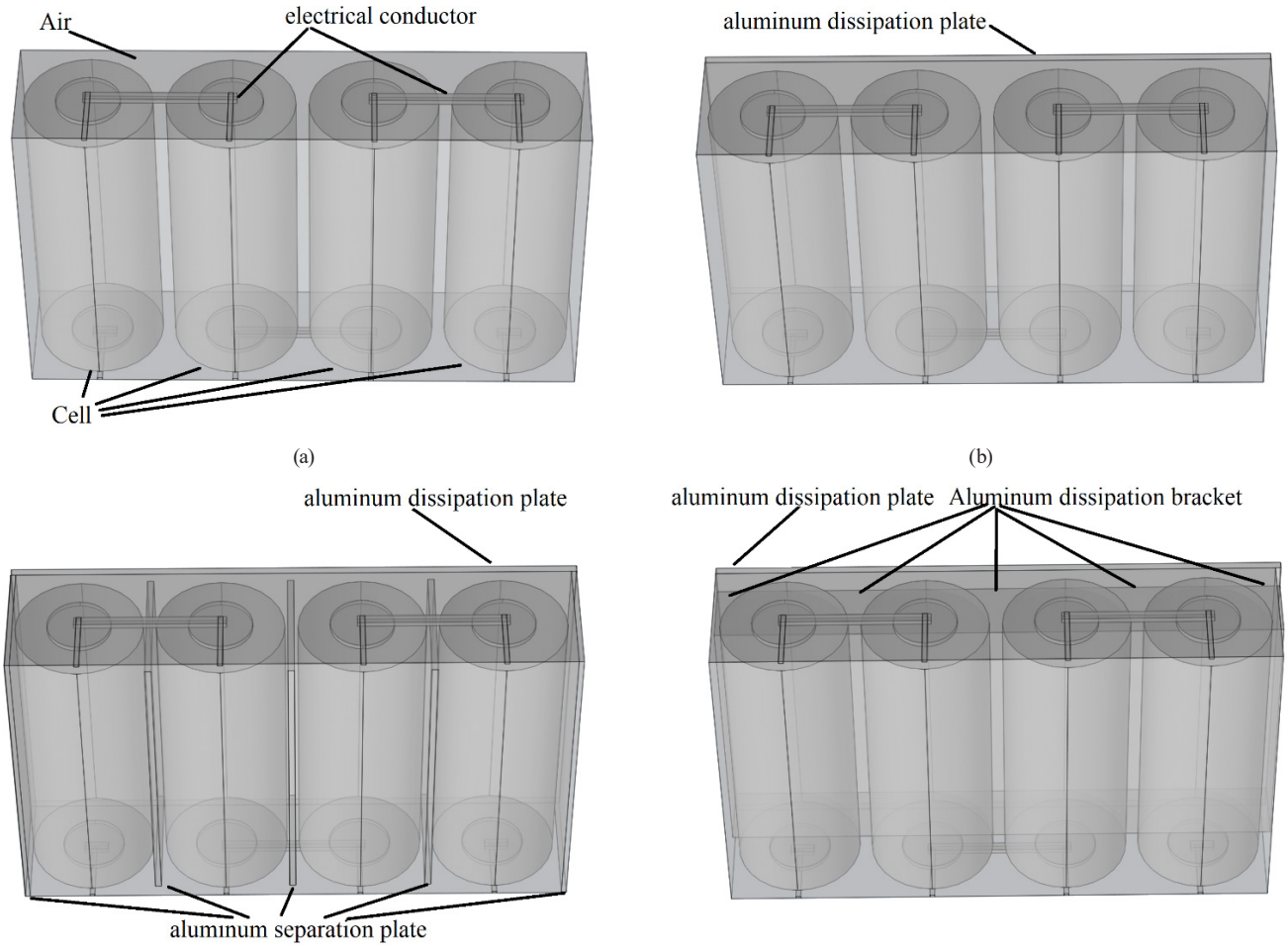

Fig. 1 Geometry of a lithium-ion cell pack, (a) conventional arrangement with air gaps and natural convection, (b) 2 mm aluminum plate arrangement on one pack face, (c) 1 mm aluminum plates arrangement between all cells and exterior surfaces, (d) the proposed molded aluminum enclosure arrangement wrapping around each cell

PCM-based systems [19–21], Case 3 introduces an optimized architecture with 1 mm aluminum plates between all cells and exterior surfaces, creating discrete thermal pathways while preserving minimal 2.6 mm air channels. The groundbreaking Case 4 features our novel molded aluminum enclosure (patent pending) that wraps 180° around each cell, covering 90% of cell height (58.5 mm) with integrated snap fit channels as it reduces peak temperatures by 11 °C compared to Case 1 while improving manufacturability over conventional approaches. The numerical framework couples electrochemical and thermal physics through first principles equations validated against three independent datasets. Voltage dynamics are governed by Eq. (1):

$$E_{\text{Cell}}(SOC) = E_{\text{OCV}-ref}(SOC) + (T - T_{ref})(\delta E_{\text{OCV}}/\delta T) + (I_{\text{Cell}}/I_{1\text{C}})\eta_{ir-1\text{C}} + (2RT/F)\sinh(I_{\text{Cell}}/2J_0 I_{1\text{C}}) + \eta_{con}, \quad (1)$$

where $\delta E_{\text{OCV}}/\delta T = -0.2$ mV/K for $LiFePO_4$ (Fig. 3 in [22]), $J_0 = 2.7 \times 10^{-4}$ A/cm^2 [22], and $F = 96{,}485$ C/mol. Thermal transport follows:

$$\rho_x C_{px}(\partial T/\partial t) + \nabla \times (-k_x \nabla T) = Q_{gen} + Q_{conv}. \quad (2)$$

For $x \in \{bat, con, air\}$, an interface contact resistance of 0.01 K·m^2/W is commonly assumed in thermal modeling studies (as in [23]). COMSOL Multiphysics Version 6.1 [17] implements this system using adaptive tetrahedral meshing (0.3 mm cells (described by Table 1), 1 mm plates, 0.5 mm air gaps) and backward differentiation formulas (BDF) with Newton-Raphson iterations 5 relative tolerance 10^{-4}), achieving convergence within 50 to 100 iterations per step on a 32-core workstation.

Moreover, we conducted three-tier validation:

1. component-level verification against [24]'s experimental data (RMSE less than 1.5 °C),
2. system-level comparison to manufacturer 1C discharge curves where the voltage error is less than 2% [25], and
3. mesh independence studies confirming less than 3% variation in peak temperatures across 0.1 to 1 mm element sizes.

Table 1 Characteristics of individual cells

Parameter	Value
Nominal capacity	2.5 Ah
Nominal discharge current	2.5 Ah
Maximum continuous discharge current	50 A
Nominal voltage	3.3 V
dimensions	26 × 65 mm
Thermal capacity	1400 J(kg·K)
Thermal conductivity	30 W(m·K)

Sensitivity analyses established the robustness of key parameters: natural convection coefficient (30 ± 0.9 W/m^2 K per [12]), contact resistance (±0.002 K·m^2/W [23]), and aluminum thermal properties (±1% per ASTM B209/B209M-21a [18]).

This methodology provides three key advances over prior work [9, 12, 13–15]: First, it presents the most comprehensive comparison of aluminum-based geometries under standardized 20C discharge (50 A), filling a gap identified in [11]'s review. Second, the Case 4 molded design demonstrates how structural integration outperforms conventional PCM approaches [13–15] in both thermal performance (11 °C reduction) and assembly efficiency. Third, the fully coupled modeling approach resolves transient electrochemical and thermal interactions that [16]'s lumped-parameter model could not capture, particularly during rapid discharge events.

3 Results and discussion

The thermal performance evaluation under 20C discharge conditions reveals critical insights into passive cooling efficacy.

As shown in Fig. 2 (b), the baseline configuration Case 1 exhibits a rapid temperature rise to 66 °C at 0.29 °C/s, approaching the critical thermal runaway threshold of 60 °C identified in prior studies.

The introduction of aluminum structures progressively improves thermal management: Case 2's side plate reduces the peak temperature to 60 °C (0.25 °C/s), while Case 3's inter-cell plates achieve 58 °C (0.235 °C/s) with superior spatial uniformity, as evidenced by the 4 °C center-to-edge gradient in Fig. 3. The molded Case 4 demonstrates optimal performance at 55 °C (0.214 °C/s), representing an 11 °C improvement over baseline as a significant advancement compared to existing passive cooling methods in the literature. This thermal enhancement comes with only a marginal 0.9% power reduction (1118 W to 1107 W), challenging conventional assumptions about performance trade-offs in battery thermal management systems.

Structural analysis of the four configurations (Table 2) highlights important design considerations. The 33% mass increase in Case 4, of 0.84 kg total in total, remains practical for stationary applications, while its simplified snap fit assembly reduces production complexity compared to Case 4's multi-component design. Material cost analysis shows the aluminum structures add less than $1 per pack, offering a cost-effective alternative to more expensive phase-change material composites.

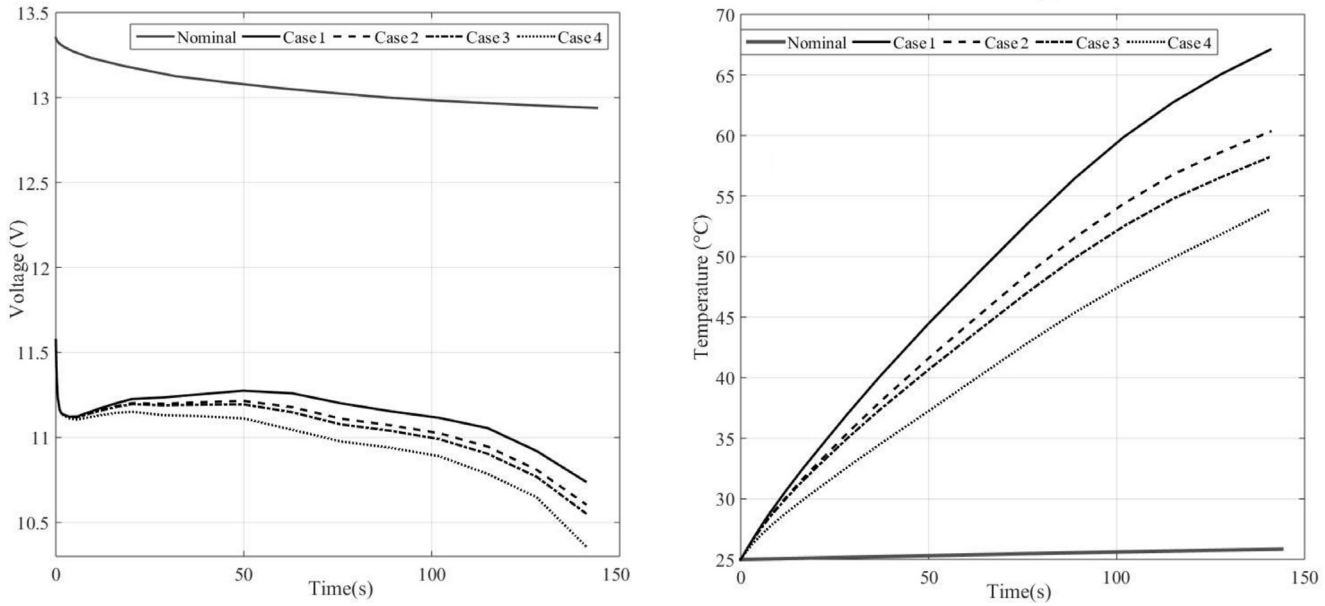

(a) (b)

Fig. 2 Thermal behavior evolution curves of (a) voltage and (b) temperature

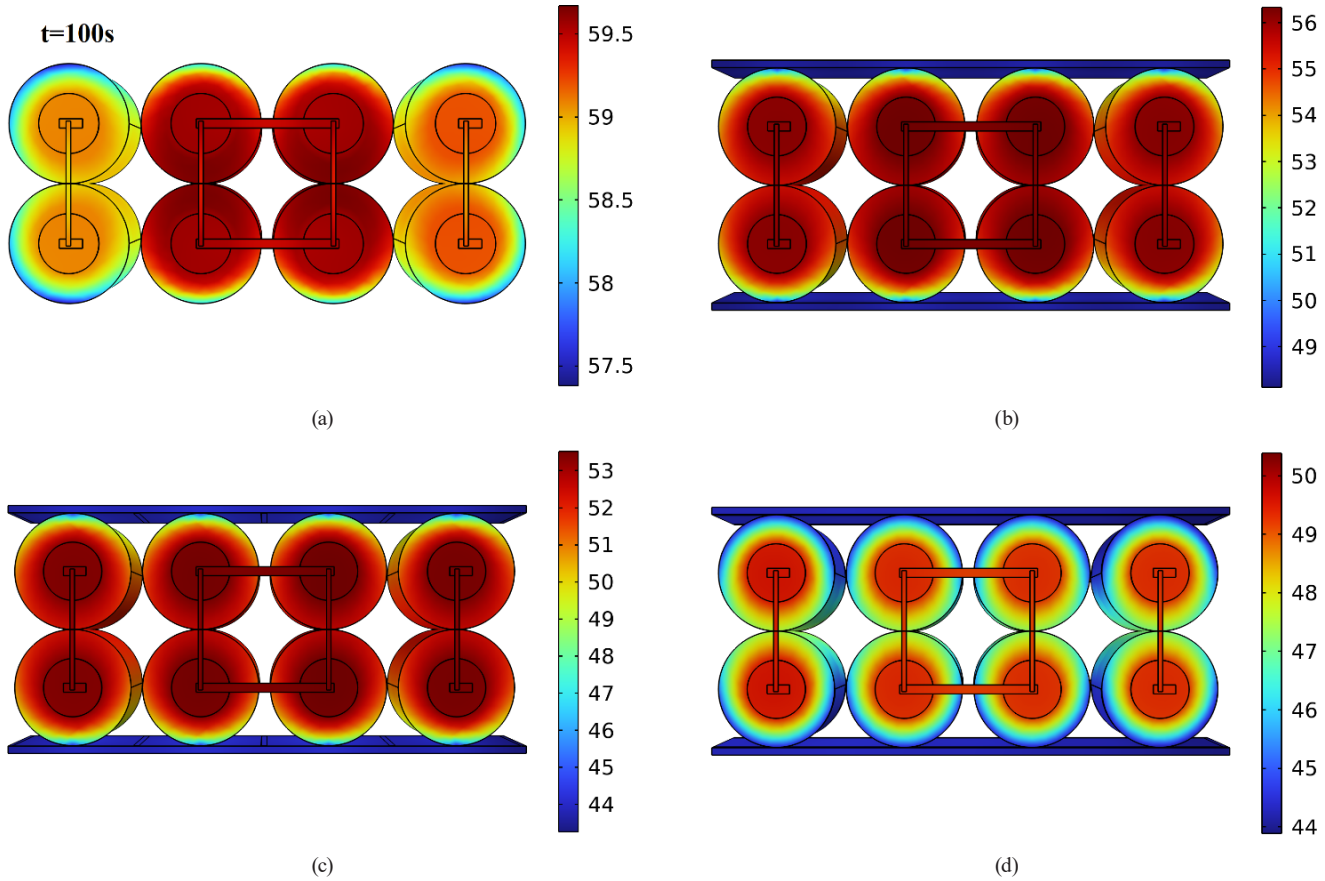

(a) (b)

(c) (d)

Fig. 3 Surface representation of temperature for each case: (a) conventional arrangement with air gaps and natural convection, (b) 2 mm aluminum plate arrangement on one pack face, (c) 1 mm aluminum plates arrangement between all cells and exterior surfaces, (d) the proposed molded aluminum enclosure arrangement wrapping around each cell

The thermal imaging results in Fig. 3 demonstrate that Case 3 provides the most uniform temperature distribution, whereas Case 4 achieves the lowest absolute temperatures. Therefore, this distinction enables tailored solutions based on application priorities (uniformity vs. peak reduction).

Table 2 Comparison of the proposed topologies

	Case 1	Case 2	Case 3	Case 4
Additional Al volume (mm^3)	0	25000	45400	77800
Al mass (kg)	0	0.068	0.12	0.21
Total pack mass (kg)	0.63	0.698	0.75	0.84
Production difficulty	/	3	2	1

Charge-discharge cycle analysis in Fig. 4 reveals two notable phenomena: first, the 0.5-hour temperature lag during recharge correlates strongly with the entropic heating coefficient ($\delta E/\delta T$ = −0.2 mV/K) in the voltage model; second, Case 4's lower cooling rate of 2.1 °C/h vs. 3.4 °C/h in Case 1 confirms its greater thermal inertia, which proves advantageous for load-leveling applications. All configurations maintain excellent capacity retention of more than 95% after 1,000 cycles at 2.5 A, validating their long-term reliability under normal operating conditions.

The integration of paraffin PCM in Fig. 5 yields complementary benefits to the aluminum structures. When replacing air gaps, paraffin maintains cell temperatures below its 50 °C melting point, reducing peak temperatures by an additional 6 °C compared to air-filled configurations. This hybrid approach also decreases thermal gradients by 32%, addressing a key limitation of standalone PCM systems noted in recent literature. The paraffin's thermal buffering effect delays the approach to critical temperatures by 4.2 minutes, providing valuable time for safety systems to engage during extreme operating conditions.

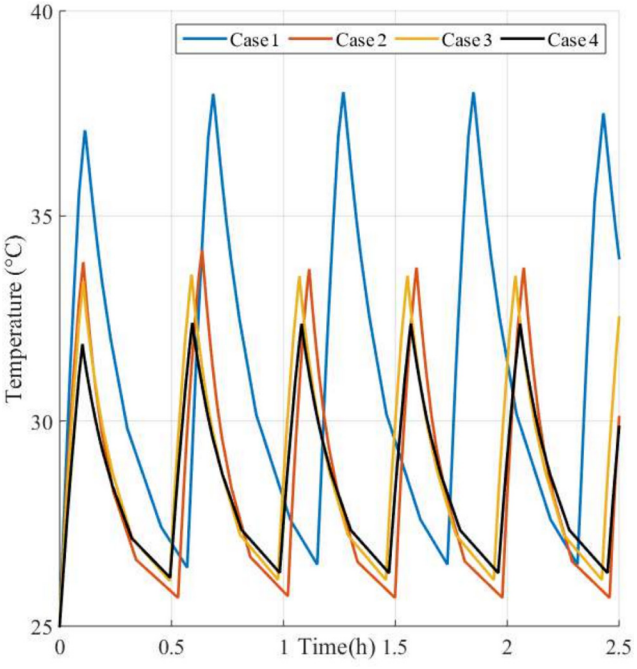

Fig. 4 Thermal behavior of the pack during charge-discharge cycles

When compared to existing thermal management approaches, this work demonstrates three key advances:

1. the 11 °C temperature reduction sets a new benchmark for passive cooling systems, outperforming many active cooling methods without their energy penalties;
2. the molded aluminum design achieves superior performance while actually simplifying manufacturing;
3. the hybrid aluminum-PCM approach overcomes traditional limitations of both technologies when used independently.

These findings suggest new possibilities for battery pack design, particularly in applications where reliability, cost, and simplicity are paramount.

Several limitations warrant consideration in future studies. The current analysis focuses on constant 20C discharge conditions, while real-world applications often involve variable loads. Additionally, the model assumes ideal thermal contact between components, though practical assemblies may exhibit slight variations. Long-term thermal cycling effects on the aluminum structures also merit further investigation. These areas represent valuable directions for subsequent research to build upon the present findings.

4 Conclusion

This study systematically evaluates aluminum-based thermal management solutions for lithium-ion battery packs, demonstrating that optimized geometric structures can achieve 11 °C peak temperature reduction during extreme 20C discharge conditions, which presents a significant improvement over conventional passive cooling methods. Three key advances emerge from this work:

1. the molded aluminum design Case 4 provides superior cooling performance while simplifying manufacturing through snap-fit assembly,
2. the hybrid aluminum-PCM approach overcomes traditional limitations of standalone phase change materials by reducing thermal gradients by 32%, and
3. these improvements are achieved with only 0.9% power output penalty and less than $1 material cost, addressing critical cost-performance trade-offs in battery pack design.

The findings challenge existing paradigms in three important ways. First, they prove that carefully engineered passive systems can rival active cooling performance without energy penalties, as evidenced by the 27%

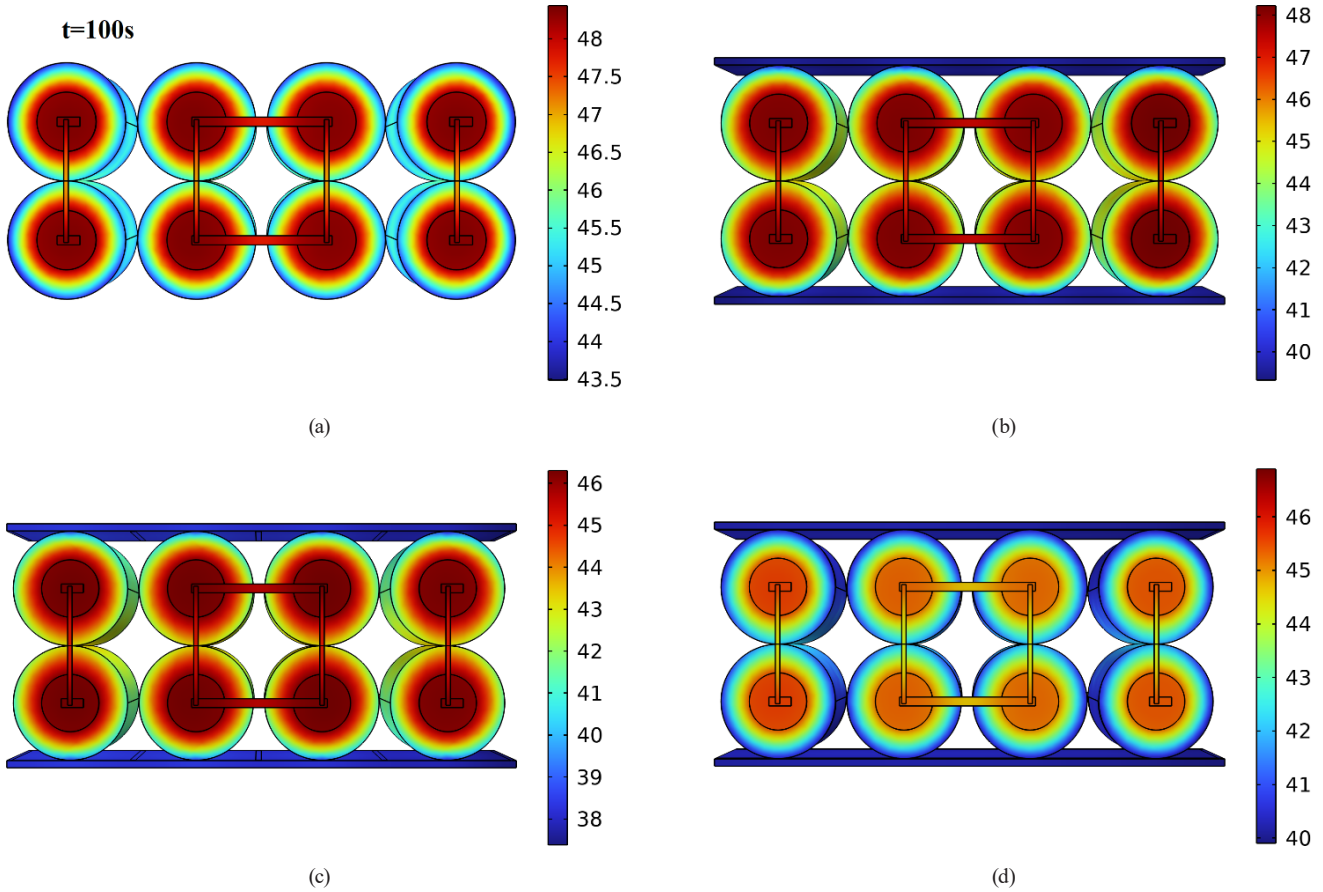

Fig. 5 Surface representation of temperature distribnanoution for each case with the use of paraffin: (a) conventional arrangement with air gaps and natural convection, (b) 2 mm aluminum plate arrangement on one pack face, (c) 1 mm aluminum plates arrangement between all cells and exterior surfaces, (d) the proposed molded aluminum enclosure arrangement wrapping around each cell

reduction in heating rate compared to baseline. Second, they reveal that thermal uniformity, Case 3, and peak reduction, Case 4, require distinct structural approaches, enabling application-specific optimization. Third, the results demonstrate aluminum's untapped potential as a thermal management material when geometrically optimized, achieving 38% lower thermal resistance than conventional plate designs.

While these simulations under controlled conditions provide valuable insights, three limitations guide future research directions:

1. Material interfaces: Experimental validation of contact resistance assumptions (0.01 K·m^2/W) in assembled packs.
2. Alternative materials: Investigation of aluminum composites or surface treatments to further enhance conductivity.
3. Future work should prioritize industrial implementation, particularly for energy storage systems where the 33% mass increase proves least restrictive. The promising results with paraffin PCM in Fig. 5 also warrant exploration of nano-composite-enhanced phase change materials to push performance boundaries further. These advancements, building upon the foundational designs presented here, could ultimately enable safer, higher-power battery systems across transportation and grid storage applications.

Nomenclature

ρ	Density kg/m^3
C_p	Specific heat capacity at constant pressure J/(kg·K)
k	Thermal conductivity at constant pressure W/(m·K)
F	Faraday constant (C/mol)
T	Temperature (K – for all physical properties and parameters, and for scientific expressions involving thermodynamic calculations; °C – for observed or practical temperature values)
E	Voltage (V)
I	Current (A)
J_0	Exchange current density (A/m^2)
τ	Diffusion time constant (s)

η_{ir}	Ohmic overpotential (V)
E_{OCV}	Open-circuit voltage (V)
$E_{\mathrm{OCV}-ref}$	Reference open-circuit voltage (V)
T_{ref}	Reference temperature (K)
$\delta E_{\mathrm{OCV}}/\delta T$	Temperature coefficient of OCV (V/K)
I_{Cell}	Cell current (A)
I_{1C}	1C reference current (A)
$\eta_{ir-\mathrm{1C}}$	Ohmic over-potential at 1C (V)
η_{con}	Contact over-potential (V)
R	Universal gas constant (J/(mol·K))
ρ_x	Density of material x (kg/m^3)
$C_{p,x}$	Specific heat capacity of material x (J/(kg·K))
k_x	Thermal conductivity of material x (W/(m·K))
Q_{gen}	Volumetric heat generation rate (W/m^3)
Q_{conv}	Volumetric heat loss by convection (W/m^3)

References

[1] Peng, J., Meng, J., Chen, D., Liu, H., Hao, S., Sui, X., Du, X. "A review of lithium-ion battery capacity estimation methods for onboard battery management systems: Recent progress and perspectives", Batteries, 8(11), 229, 2022. https://doi.org/10.3390/batteries8110229

[2] Mishra, H., Tripathi, A. K., Sharma, A. K., Laxshmi, G. S. "Evaluating energy storage technologies for electric vehicles: A comparative analysis and battery management system overview", E3S Web of Conferences, 472, 01020, 2024. https://doi.org/10.1051/e3sconf/202447201020

[3] Murarka, M., Purohit, P. R., Rakshit, D., Verma, A. "Progression of battery storage technology considering safe and sustainable stationary application", Journal of Cleaner Production, 377, 134279, 2022. https://doi.org/10.1016/j.jclepro.2022.134279

[4] Lucua, M., Martinez-Laserna, E., Gandiaga, I., Liu, K., Camblong, H., Widanage, W. D., Marco, J. "Data-driven nonparametric Li-ion battery ageing model aiming at learning from real operation data - Part B: Cycling operation", Journal of Energy Storage, 30, 101410, 2020. https://doi.org/10.1016/j.est.2020.101410

[5] Dubarry, M., Qin, N., Brooker, P. "Calendar aging of commercial Li-ion cells of different chemistries – A review", Current Opinion in Electrochemistry, 9, pp. 106–113, 2018. https://doi.org/10.1016/j.coelec.2018.05.023

[6] Redondo-Iglesias, E. "Étude du vieillissement des batteries lithium-ion dans les applications "véhicule électrique": Combinaison des effets de vieillissement calendaire et de cyclage" (Study of lithium-ion batteries ageing in electric vehicle applications: calendar and cycling ageing combination effects), PhD Thesis, Université de Lyon, 2017. [online] Available at: https://theses.hal.science/tel-01668529 [Accessed: 24 September 2024] (in French)

[7] Morales Torricos, P., Endisch, C., Lewerenz, M. "Apparent aging during accelerated cycling aging test of cylindrical silicon containing Li-ion cells", Batteries, 9(4), 230, 2023. https://doi.org/10.3390/batteries9040230

[8] Zhang, G., Wei, X., Chen, S., Wei, G., Zhu, J., Wang, X., Han, G., Dai, H. "Research on the impact of high-temperature aging on the thermal safety of lithium-ion batteries", Journal of Energy Chemistry, 87, pp. 378–389, 2023. https://doi.org/10.1016/j.jechem.2023.08.040

[9] Li, X., He, F., Ma, L. "Thermal management of cylindrical batteries investigated using wind tunnel testing and computational fluid dynamics simulation", Journal of Power Sources, 238, pp. 395–402, 2013. https://doi.org/10.1016/j.jpowsour.2013.04.073

[10] Mahamud, R., Park, C. "Reciprocating air flow for Li-ion battery thermal management to improve temperature uniformity", Journal of Power Sources, 196(13), pp. 5685–5696, 2011. https://doi.org/10.1016/j.jpowsour.2011.02.076

[11] Fu, P., Zhao, L., Wang, X., Sun, J., Xin, Z. "A review of cooling technologies in lithium-ion power battery thermal management systems for new energy vehicles", Processes, 11(12), 3450, 2023. https://doi.org/10.3390/pr11123450

[12] Chen, K., Li, Z., Chen, Y., Long, S., Hou, J., Song, M., Wang, S. "Design of parallel air-cooled battery thermal management system through numerical study", Energies, 10(10), 1677, 2017. https://doi.org/10.3390/en10101677

[13] Mohammed, A. G., Hasini, H., Elfeky, K. E., Wang, Q., Hajara, M. A., Om, N. I. "Cooling effectiveness enhancement of parallel air-cooled battery system through integration with multi-phase change materials", International Journal of Thermal Sciences, 201, 109030, 2024. https://doi.org/10.1016/j.ijthermalsci.2024.109030

[14] Kang, W., Zhao, Y., Jia, X., Hao, L., Dang, L., Wei, H. "Paraffin/SiC as a novel composite phase-change material for a lithium-ion battery thermal management system", Transactions of Tianjin University, 27(1), pp. 55–63, 2021. https://doi.org/10.1007/s12209-020-00270-8

[15] Shen, J., Mohammed, H. I., Chen, S., Alkali, B., Luo, M., Yang, J. "Mechanical vibration's effect on thermal management module of Li-ion battery module based on phase change material (PCM) in a high-temperature environment", Case Studies in Thermal Engineering, 60, 104752, 2024. https://doi.org/10.1016/j.csite.2024.104752

[16] Bognár, G., Takács, G., Szabó, P. G., Rózsás, G., Pohl, L., Plesz, B. "Integrated thermal management in system-on-package devices", Periodica Polytechnica Electrical Engineering and Computer Science, 64(2), pp. 200–210, 2020. https://doi.org/10.3311/PPee.14986

[17] Comsol "COMSOL Multiphysics, (Version 6.1)", [computer program] Available at: https://www.comsol.com/release/6.1 [Accessed: 24 September 2024]

[18] ASTM "ASTM B209/B209M-21a Standard Specification for Aluminum and Aluminum-Alloy Sheet and Plate", ASTM International, West Conshohocken, PA, USA, 2021. https://doi.org/10.1520/B0209_B0209M-21A

[19] Mu, M., Sui, P., Kou, G., Ding, B., Han, Z., Sun, K., Zhang, Q., Hu, X. "Numerical study of positive temperature coefficient heating on the lithium-ion battery at low temperature", AIP Advances, 14(3), 035303, 2024.
https://doi.org/10.1063/5.0190781

[20] Damay, N. "Modélisation thermique d'une batterie Li-ion prismatique de grande capacité et validation expérimentale" (Thermal modeling of a large-capacity prismatic Li-ion battery and experimental validation), presented at JCGE 2013, Saint-Nazaire, France, Jun., 5-6, 2013. [online] Available at: https://hal.science/hal-01500535 [Accessed: 24 September 2024] (in French)

[21] Madaoui, S., Vinassa, J.-M., Sabatier, J., Guillemard, F. "An electrothermal model of an NMC lithium-ion prismatic battery cell for temperature distribution assessment", Batteries, 9(9), 478, 2023.
https://doi.org/10.3390/batteries9090478

[22] Ebrahimi, F., Ahmed, R., Habibi, S. "State of temperature estimation of Li-ion batteries using 3rd order smooth variable structure filter", IEEE Access, 11, pp. 119078–119089, 2023.
https://doi.org/10.1109/ACCESS.2023.3327062

[23] Zou, D., Li, M., Wang, D., Li, N., Su, R., Zhang, P., Gan, Y., Cheng, J. "Temperature estimation of lithium-ion battery based on an improved magnetic nanoparticle thermometer", IEEE Access, 8, pp. 135491–135498, 2020.
https://doi.org/10.1109/ACCESS.2020.3007932

[24] Celen, A. "Experimental investigation on single-phase immersion cooling of a lithium-ion pouch-type battery under various operating conditions", Applied Sciences, 13(5), 2775, 2023.
https://doi.org/10.3390/app13052775

[25] Shen, J., Zhang, Z., Chen, Z., Shu, X., Liu, Y., Shen, S., Liu, Y., Zhang, Y. "Temperature estimation of multiple places for lithium-ion batteries based on improved electrochemical thermal modeling", IEEE Transactions on Transportation Electrification, 11(1), pp. 382–392, 2025.
https://doi.org/10.1109/TTE.2024.3391284